LRP 367/88 November 1988

OPTICAL DIAGNOSIS OF ELECTROSTATIC WAVES IN THE ION GYROFREQUENCY RANGE VIA THE ION DIELECTRIC RESPONSE

T.N. Good, F. Skiff, F. Anderegg, P.J. Paris, M.Q. Tran,
N. Rynn and R.A. Stern

Contributed Paper presented by

T.N. Good

at the

International Workshop "Nonlinear Phenomena in Vlasov Plasmas"
July 11 - 16, 1988
Cargèse, Corsica - France

OPTICAL DIAGNOSIS OF PLASMA WAVES VIA THE ION DIELECTRIC RESPONSE

T.N. Good, F. Skiff, F. Anderegg, P.J. Paris,
M.Q. Tran, N. Rynn+ and R. Stern*

Centre de Recherches en Physique des Plasmas
Association Euratom - Confédération Suisse
Ecole Polytechnique Fédérale de Lausanne
21, Av. des Bains/CH-1007 Lausanne/Switzerland

+ University of California, Irvine, CA
* University of Colorado, Boulder, CO

ABSTRACT

We present experiments that utilize Laser Induced Fluorescence (LIF) measurements of a component of the perturbed ion velocity distribution in the fields of externally excited electrostatic waves with frequencies near the ion cyclotron frequency. We show that the distribution function oscillates coherently at the wave frequency, and that a linear analysis of these coherent fluctuations allows a determination of wave characteristics such as the electric field amplitude and wave vector. Three methods are described which directly indicate wave properties via the perturbed ion distribution, $f^{(1)}(v,x,t)$ and the zero and first order moments of $f^{(1)}(v,x,t)$. We demonstrate that this non-perturbative diagnostic is a powerful tool in the study of wave excitation and wave particle interactions.

I. Introduction

Laser induced fluorescence (LIF) has been demonstrated to be a sensitive non-perturbative diagnostic of ion kinetics. LIF is widely used to measure the ion velocity distribution function and moments of the distribution such as density, drift velocity and temperature.[1,2,3] It is further employed to determine ion transport properties in phase space under a variety of plasma conditions ranging from quiescence to strong wave-particle interaction.[4,5,6] In the latter, considerable information about the wave fields is contained in the particle distributions.[7,8,9]

This paper presents the results of an experimental investigation, utilizing LIF, of electrostatic waves near the ion cyclotron frequency, namely the electrostatic ion cyclotron (EIC) wave and the neutralized ion Bernstein (NIB) wave. Through the use of phase-lock techniques, or local measurements of the ion distribution synchronous with the wave field, a component of the perturbed distribution is observed that oscillates coherently with the wave.

Three methods are decribed below. In the first method a component of the perturbed ion velocity distribution $f^{(1)}(v_y,x;t)$ is measured at a single point in space. For finite $k_x\rho$, this method yields the electric field amplitude, while for $k_x\rho \geq 1.5$ a fourier transform of $f^{(1)}$ with respect to v_y gives the k spectrum of the ion response. Detailed structure in $f^{(1)}$ is found only for waves having a phase velocity on the order of the ion thermal speed.

The second method utilizes the zero order moment of $f^{(1)}(v_y)$, i.e. the perturbed density fluctuations. By scanning the laser in space and time, we determine wavelength, amplitude, propagation, and dispersion characteristics. This method is limited to electrostatic waves with a net $\delta n/n_0 = \int f^{(1)}(v_y)dv_y / \int f^{(0)}(v_y)dv_y$.

The third method takes the first order moment of $f^{(1)}(v_y)$ to get an average ion drift velocity, or ion current, transverse to k, $\langle v_y \rangle = \int f^{(1)}(v_y) v_y dv_y$. In this case, a scan in space yields a measure of wavelength and wave amplitude. This method can also be applied to electromagnetic waves which exhibit a transverse ion velocity response.

The application of all the three methods is subject to the limitation of diagnosis of waves with frequency less than or about the ion plasma frequency, and with wavelength greater than the diagnosed plasma volume defined by the intersection of the laser beam and the focal image of the fluorescence detection optics. Methods 1 and 3 require the use of a narrow bandwidth laser, while method 2 allows use of a laser bandwidth much broader than the Doppler broadened ion absorption linewidth.

II. Theory

In order to develop a theoretical expression for the perturbed component of the ion velocity distribution in the presence of an electrostatic wave we consider the Vlasov equation :

$$\frac{\delta f}{\delta t} + \mathbf{v} \bullet \nabla_x f + \frac{e}{m}(\mathbf{E} + \frac{\mathbf{v}}{c} \mathrm{x}\, \mathbf{B}) \bullet \nabla_v f = 0 \qquad \text{equation (1)}$$

Treating the electric field as a perturbation, we linearize the distribution,

$$f = f^{(0)} + f^{(1)} + f^{(2)} + \ldots\ldots \qquad \text{equation (2)}$$

and solve the linearized equation for $f^{(1)}$, to obtain[7] :

$$f^{(1)}(v_y, \mathbf{x}; t) = \frac{-e\phi(\mathbf{x}, t)}{mv_t^2}\,\zeta_0 e^{ia}\sum_{n,m} J_m(a) I_n\left(\frac{\lambda}{4}\right) e^{\frac{-\lambda - im2\pi}{4}}\, Z(\zeta_{2n+m})\bullet f^{(0)}(v_y)$$

equation (3)

where we have integrated over a velocity components in the plane defined by k and the externally imposed magnetic field, B, (v_x and v_z) and we have used the following variable definitions :

$$\mathbf{E} = -\nabla\ \phi \qquad \phi = \phi_0 e^{i\mathbf{k}_x \bullet \mathbf{x} + ik_{\|} z - i\omega t} \qquad \zeta_n = \frac{\omega - n\Omega}{\sqrt{2}\, k_{\|} v_t}$$

$$a \equiv \frac{k_x v_y}{\Omega} \qquad \lambda \equiv \left(\frac{k_x v_t}{\Omega}\right)^2$$

For a propagating wave, the parameters appearing in eq. (4) will not be arbitrary, but will be constrained by the electrostatic dispersion relation.

The average ion velocity is given by :

$$\begin{aligned} \langle v_y \rangle &= \int_{-\infty}^{\infty} v_y f^{(1)}(v_y)\, dv_y \\ &= M_{yx} E_x + M_{yz} E_z \\ &= c\frac{E_x}{B_0} \sum_n \zeta_0 Z(\zeta_n) \frac{d}{d\lambda} [I_n(\lambda) e^{-\lambda}] \end{aligned}$$

equation (4)

where Mi,j are the off-diagonal elements of the ion mobility tensor.[7]

III. Experimental Results

In order to test the predictions of the formulas derived above, electrostatic waves in the ion gyrofrequency range were generated in an argon discharge plasma,[7] and in a Q-machine barium plasma,[10] in the LMP device.[11] Plasma densities were of the order 10^9-10^{11}, T_i=0.1-0.2 eV, T_e=10 eV for the argon discharge and $T_e=T_i$ for the barium plasma, and B was variable between 1-3 kGauss. The optical diagnostic system of the LMP includes a pulsed eximer pumped dye laser and a CW argon pumped dye laser. Beam steering and detection optics allow scanning of the plasma volume along and across the magnetic field.[12] Ionic transitions from the ground and metastable states of barium were excited by absorption of laser radiation at 493.4 nm and 585.4 nm, respectively, and from an argon metastable state via radiation at 611 nm.

Figure 1 shows measurements of the perturbed barium ion distribution at $\pi/2$ increments of the wave phase, as well as the unperturbed ion velocity distribution. Also shown is the perturbed distribution derived from eq. (3) subject to the parameters found from the roots of the dispersion function. Figure 1 demonstrates the "breathing", or coherent fluctuations of the distribution in an EIC wave period.

The average argon ion current was measured under conditions where both the EIC and NIB waves were excited. Figure 2 (taken from reference 7) shows a plot of the average velocity vs. radial position, as a snapshot in time. A solid line is drawn through the data points and a dashed line represents the anticipated EIC wavelength. In the bottom of Fig. 2 we show the electric field profile of the NIB wave calculated by use of the electrostatic wave equation and the relevant geometric considerations imposed by the antenna.

Method 2 is illustrated by figures 3,4, and 5. In Fig. 3 we display perpendicular scans of the perturbed ion density at various times in the EIC wave period. This data determines the wave vector in the plane normal to B. Figure 4 shows scans of $\delta n/n_0$ along the magnetic field for various wave frequencies. A study of this kind, covering a complete range of frequencies, allows a determination of the plasma dispersion relation. At the bottom of this figure we show a plot of the real and imaginary components of the density response corresponding to $f/f_{ci}=3.2$, as the optical probe is scanned along the magnetic field. The spiraling nature of the plot indicates pure propagation accompanied by a spacial damping of the mode. By fixing the position and time of measurement, and scanning the antenna frequency we investigate the frequency dependence of the ion response to the antenna structure, see Fig. 5. This method proves useful when testing antenna designs with variable ring spacing or phasing.

IV. Conclusions and Proposals

Information about plasma waves contained in the ion velocity distribution may be extracted from LIF measurements, a non-perturbative diagnostic. A test of the linear Vlasov theory predictions has been performed, showing good agreement of theory and experiment.

Having proven the principle of this method, we propose a comprehensive test of linear theory, including dispersion characteristics and Landau damping. Furthermore, a study of non-linear effects under large amplitude single wave excitation is suggested where $f^{(2)}(v, x;t)$ would yield information about harmonic generation and parametric decay processes. Lastly, the ion response may be studied in the case of two wave excitation, by investigating the coherent oscillations at the beat frequencies of the two waves.

References

1. T.N. Good et al., Phys. Fluids, 31, 1237 (1988).
2. F. Skiff et al, Phys. Rev. Lett., 58, 1430 (1986).
3. D.N. Hill et al, Rev. Sci. Instrum., 54, 30 (1983).
4. R. McWilliams and M. Okubo, Phys. Fluids, 30, 2849 (1987).
5. R.A. Stern et al, Phys. Lett., 93A, 127 (1983).
6. F. Skiff et al, Phys. Rev. Lett. 61, 2034 (1988)
7. F. Skiff and F. Anderegg, Phys. Rev. Lett., 59, 896 (1987).
8. R.A. Stern et al, Phys Rev. Lett., 47, 792 (1981).
9. R. McWilliams and D.P. Sheehan, Phys. Rev. Lett., 56, 2485 (1986).
10. N. Rynn, Rev. Sci. Instrum., 35, 40 (1964).
11. P. Paris and N. Rynn,"The LMP-Q, an Improved Barium Plasma Q-Machine", submitted for publication (1988).
12. F. Anderegg et al, Rev. Sci. Instrum., 59 2306 (1988).

FIGURE CAPTIONS

Fig. 1 Perturbed component of the ion velocity distribution at $\pi/2$ increments of wave phase angle. The column to the right shows measured distributions, while the column to the left shows the corresponding distributions derived from Equation (3).

Fig. 2 Transverse ion current response.

a) Snap-shot of the average transverse ion velocity in the presence of waves.

b) Prediction of the waveform from the electrostatic wave equation, both the EICW and NIBW are included.

Fig. 3 Wave interferograms in the plane perpendicular to the magnetic field. Top figure shows the unperturbed ion density profile, and succeeding scans show the perturbed ion density, at $\pi/2$ increments of wave phase.

Fig. 4 Wave interferograms in the plane parallel to the magnetic field. Wave dispersion demonstrated by scans of the perturbed ion density at various frequencies.

Fig. 5 Magnitude of perturbed ion density as the antenna frequency is scanned over a range of 0.1 - 2.5 ω/Ω_{ci}.

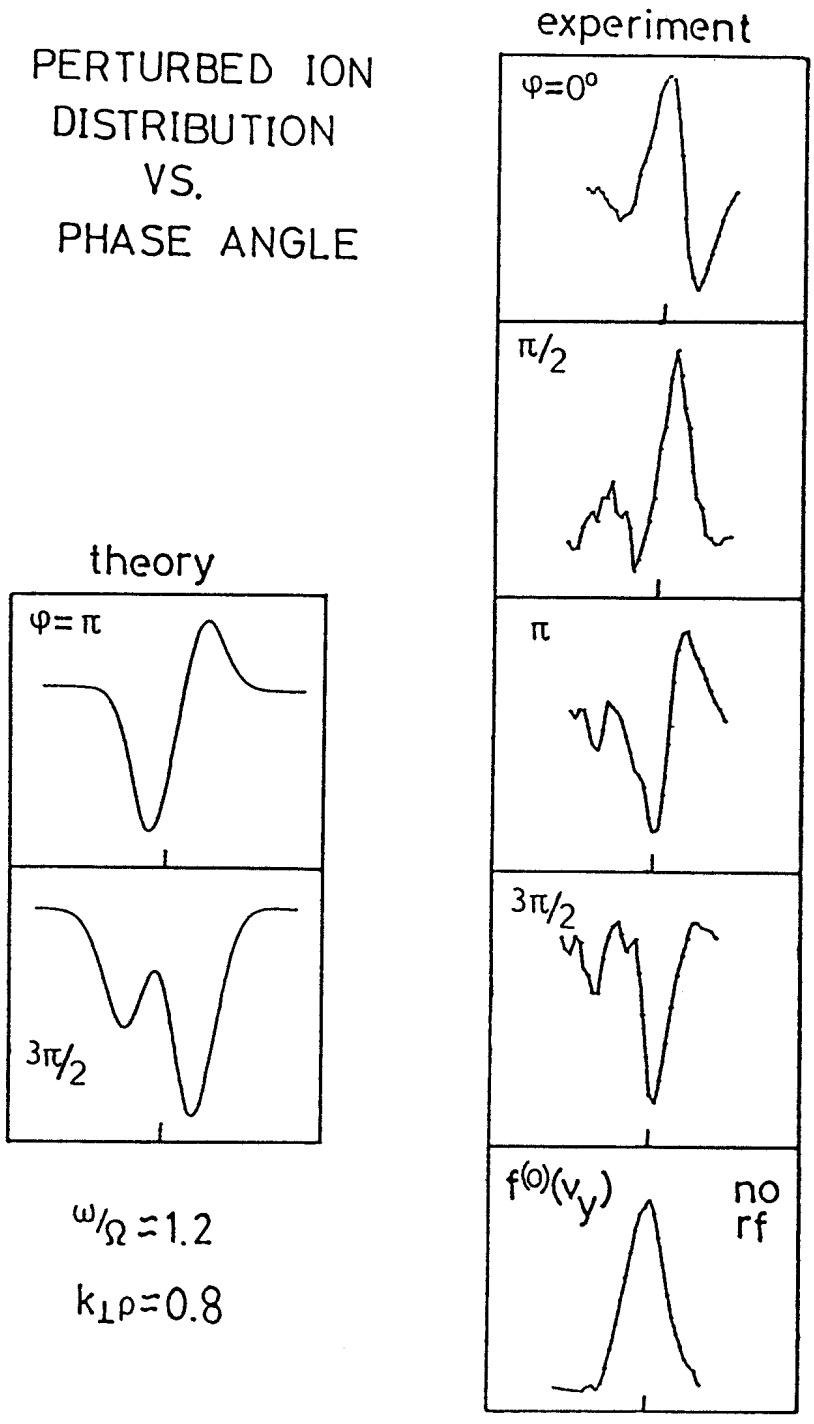
PERTURBED ION
DISTRIBUTION
VS.
PHASE ANGLE
experiment
φ=0°
π/2
π
3π/2
f(0)(vy)
no
rf
theory
φ=π
3π/2
ω/Ω=1.2
k⊥ρ=0.8

Fig. 1

a)

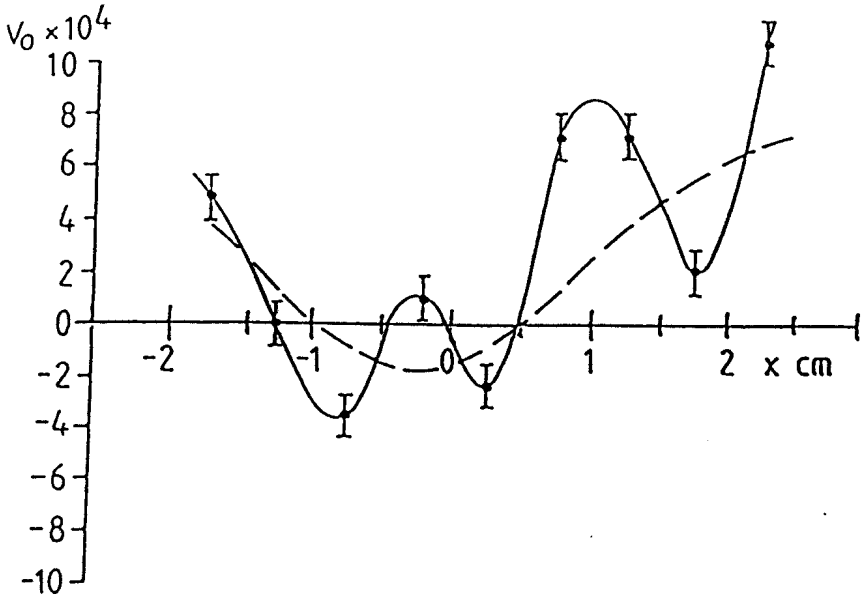

b)

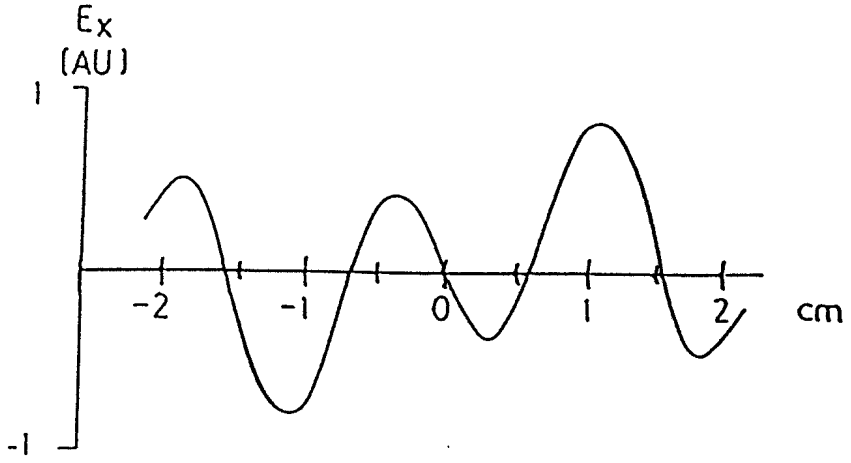

Fig. 2

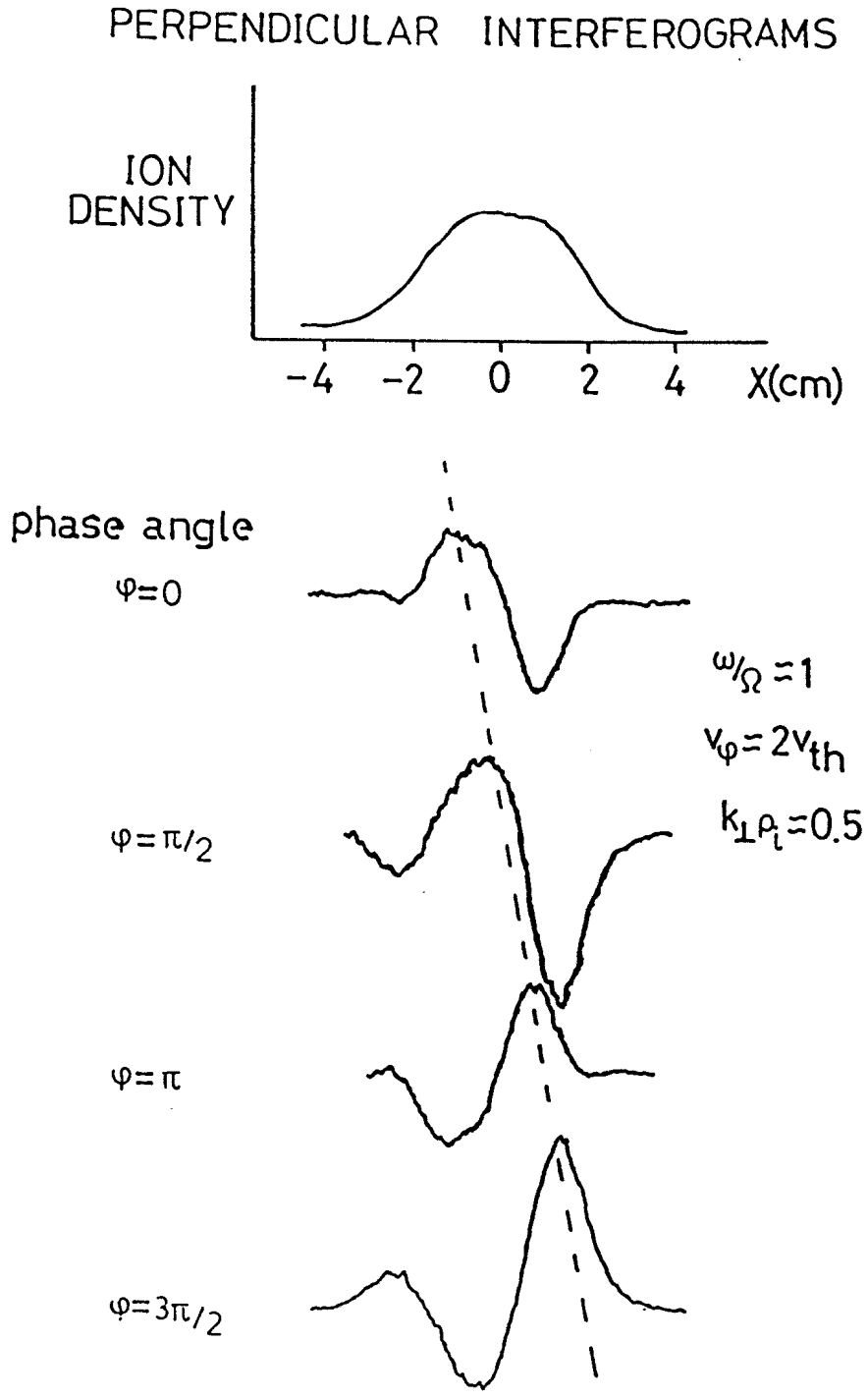
PERPENDICULAR INTERFEROGRAMS
ION DENSITY
-4
-2
0
2
4
X(cm)
phase angle
φ=0
φ=π/2
φ=π
φ=3π/2
ω/Ω=1
vφ=2vth
k⊥ρi=0.5

Fig. 3

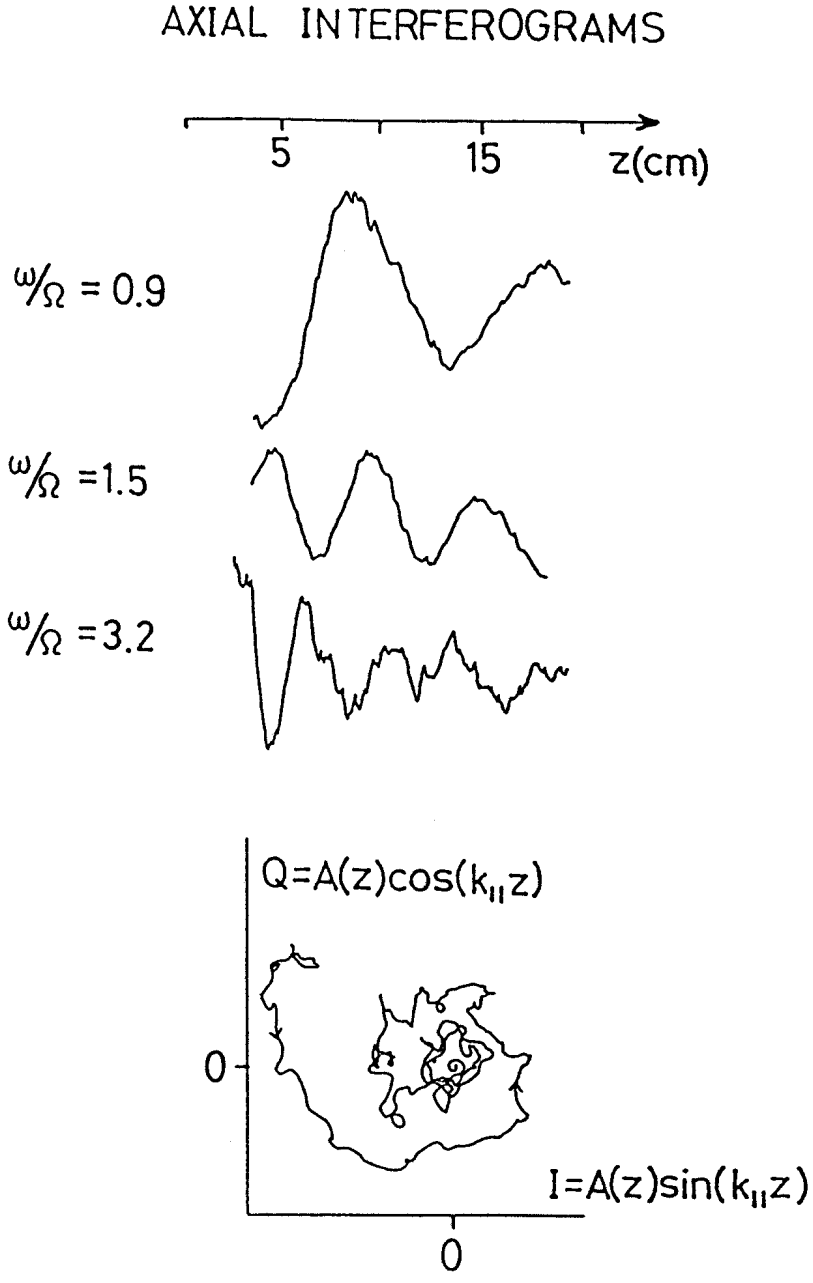
AXIAL INTERFEROGRAMS
5
15
z(cm)
ω/Ω = 0.9
ω/Ω =1.5
ω/Ω =3.2
Q=A(z)cos(k∥z)
0
I=A(z)sin(k∥z)
0

Fig. 4

ANTENNA COUPLING

ION RESPONSE VS. FREQUENCY

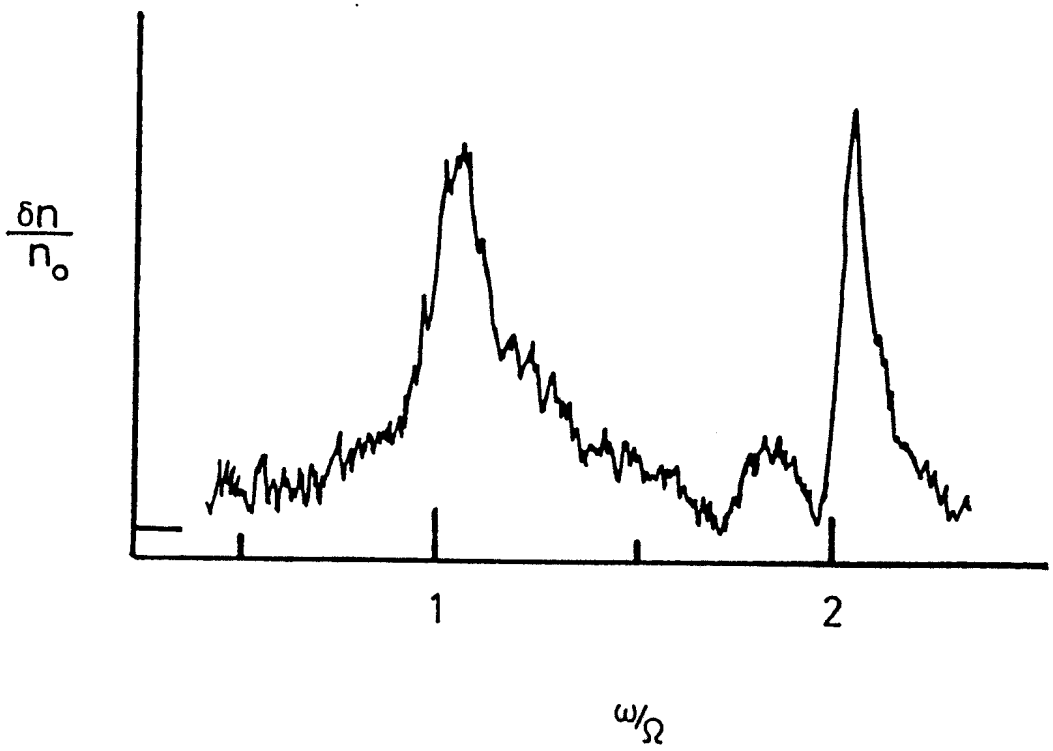

Fig. 5